Breakdown Process Experiments of Cap-and-Pin Insulators and their EMT Leader-Progression Model Implementation

F. Koehler [1*], J. Swingler [1], V. Peesapati [2]

[1] School of Engineering & Physical Sciences, Heriot-Watt University, Edinburgh, EH14 4AS, UK
[2] University of Manchester, Manchester, M13 9PL, UK
[*] fmk1@hw.ac.uk

Abstract: In this paper, breakdown tests of cap-and-pin glass insulators with arcing horns, conducted at two different HV Labs, are presented. Since only volt-time curves are measured, a curve-fitting approach to determine leader-progression-model parameters is taken, which involves modelling of the impulse generator in detail and inclusion of the Motoyama model to simulate the breakdown. Furthermore a comparison of the breakdown simulation results with LPM parameters for an air gap electrode arrangement and the measurements is accomplished. Finally a curve-fitting procedure is developed to fit the resulting volt-time-curves from simulations to the measurements.

1. Introduction

The assessment of the lightning performance of a transmission line nowadays is often performed utilizing EMT simulations. One of the most important models in such simulations is the flashover model of the insulator, because it has a major impact on the simulation results [1] and evaluation of the line flashover rate respectively. There exist several models in the literature, such as voltage-threshold-models [2], voltage-time curve models [3], disruptive effect-method [4], [5] and leader-progression models (LPM) [6]–[10] to simulate the flashover behaviour, but all lack an universal application due to their derivation. In recent time, the application of LPMs became more common, since CIGRE [11]–[13] and IEEE [3] recommend its usage due to the LPMs general application for air gaps and good agreement with measurements and IEC [14] recommends its usage for long air gaps only. Furthermore in [10] a LPM for short air gaps and transmission line arresters with air gaps (TLA) is described, which shows good agreement with the measured volt-time curves. Although the older LPM model by Pigini [7], mentioned in both CIGRE [11]–[13] and IEC [14] is still in use, the newer LPM model by Motoyama [6] has become popular in the last decade [1], [15]–[20] due to its independence of the 50% flashover voltage V_{50}, eliminating the probability element and the inclusion of the pre-discharge current into the model equivalent circuit. However, as pointed out in [17], most LPMs are based on measured breakdown data of air gaps, rather than practical insulator arrangements. Therefore in [17] the flashover behaviour of porcelain and composite insulators without arcing horns is investigated and the Motoyama LPM adapted to fit the results.

Since these investigations show, that the model parameters are unique for each type of insulator or gap arrangement, the conclusion can be drawn that in case of the investigating a whole line route, it may be beneficial to test a full set of insulator and arcing horns in the laboratory and tune the model's parameters to fit to laboratory tests to improve the evaluation of the lightning performance of this line. For transmission system operators, which deploy the same type of insulator-arcing horn set, e.g. glass or porcelain insulators with a varying number of discs, furthermore breakdown test of a range of insulators disc arrangements of the same type may be used for a scalable flashover model.

As reported in [6], [7], [17] short-tail waveshapes, as encountered during a lightning strike at the insulator, lead to a higher voltage withstand capability than the 1.2/50 µs standard waveshape. However, for most impulse generators, resistor kits are only available for standard waveshapes, such as 250/2500 µs for switching and 1.2/50 µs for lightning impulse, which restrict testing to these waveshapes. Nevertheless, in [6] it is reported, that obtained LPM parameters from short-tail impulses also fit the breakdown characteristics of standard lightning impulses. This leads to the conclusion that LPM parameters obtained with a 1.2/50 µs waveshape represent a worst-case for the breakdown behaviour of the tested insulator/ arcing horn arrangement, which adds a safety margin in the assessment of the lightning performance.

Therefore in this paper the work of determining a scalable LPM model based on [6], [17], [18] and the above discussion is presented for cap-and-pin insulators with arcing horns as a string arrangement not investigated up to now in the literature. Overall the work comprises the following:

- An implementation of the flashover model and laboratory impulse generator model alongside the flashover model's verification in an EMT software,
- conduction of laboratory tests with a 1.2/50 µs waveshape on a cap-and-pin glass insulator string with arcing horns with a various number of discs to determine the 50% flashover voltage and volt-time (V-t) curves,
- comparison of V-t-curves with generated V-t-curves using standard parameters available in the literature,
- adjustment of the LPM's parameters to fit the measured V-t-curves

2. Laboratory Breakdown Tests of Insulator-Arcing Horn Sets

To provide the data basis for the LPM parameter adjustments, breakdown tests on a cap-and-pin insulator with arcing horns are performed

2.1. Test Setup

Tests are performed at the HWU HV Lab with a Ferranti 8-stage 800 kV impulse generator with a 1.2/50 µs waveform applied at the bottom part of the string as depicted in Fig. 1 (right). The maximum number of discs to be tested is limited to 9 discs due to the generators efficiency of 95% at this waveform and limited clearance to ground due to the fixed position of the pole arm. Therefore tests are furthermore conducted at the University of Manchester High Voltage Lab, which features a Haefely 10-stage 2000 kV impulse generator with the same waveform. There, the voltage was applied at the top of the string as shown in Fig. 1(a) (left). Due to efficiency limits, the maximum number of discs is limited to 14 in this case. The cap-and-pin insulator string with arcing horns is of suspension type, where each cap-and-pin disc is of 250 mm diameter with an approximate creepage distance of 400 mm.

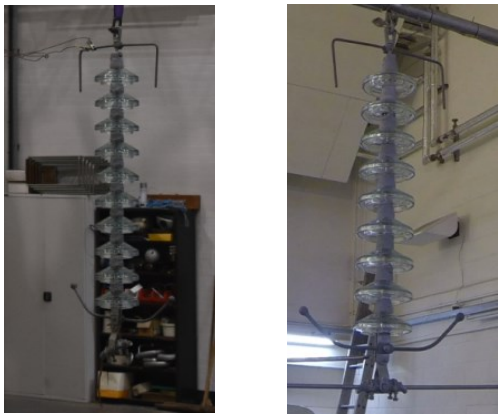

(a) *Arrangement of srings*

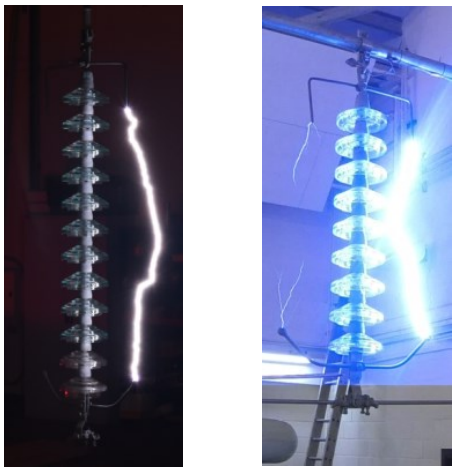

(b) *Arcing horn breakdown*

Fig. 1. *Cap-and-pin insulator string and arcing horn set, left: arrangement at UoM, right: arrangement at HWU*

2.2. 50% Flashover Voltage Measurement Results

First, the 50% flashover voltage for both positive and negative polarity is determined with the up-and-down method according to BS EN 60060-1 [21] until 10 or more flashovers occurred at 20°C and 1013 hPa for each setup. A summary of insulator test setups is provided in Table 1 alongside with pictures of the flashover tests in Fig. 1(b).

Table 1 *Test setup scenarios*

Voltage Application Point	No. of Discs	Arc Gap (m)
Bottom	5	0.43
Bottom	6	0.57
Bottom	7	0.71
Bottom	8	0.85
Bottom	9	0.99
Top	9	0.99
Top	10	1.13
Top	12	1.27
Top	14	1.41

The recorded and processed results of the determination of 50% flashover voltages are summarized in Fig. 2 and Table II. Both the positive and negative 50% flashover results for increasing number of discs show a linear behavior, whereas the difference between positive and negative 50% flashover voltage is slightly increasing with the number of discs in a string. For the 9 disc measurements, conducted both at HWU and UoM, a noticeable difference in the results exists, which is attributed to the different laboratory setups as well as the point of voltage application. As encountered during the tests, the reproducibility of negative 50% flashover results is not always constant, as seen in the coefficient of variation σ/μ in Table 2, but in general smaller than in [17].

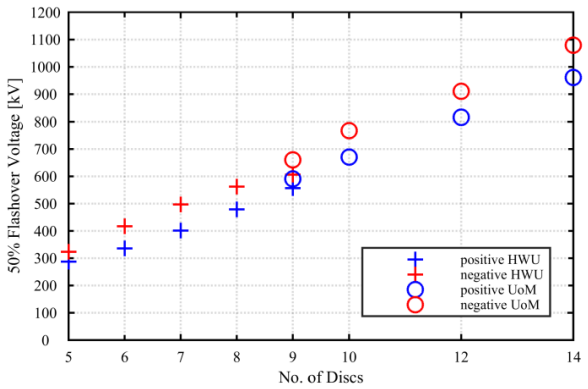

Fig. 2. *Summary of 50% flashover results with up-and-down method*

Table 2 *50% flashover results*

No. of Discs	$V_{50\%+}$ (kV)	$\sigma/\mu+$	$V_{50\%-}$ (kV)	$\sigma/\mu-$
5	288	0.0155595976	323	0.0292088258
6	336	0.0165733388	417	0.0136825789
7	401	0.0110867121	497	0.0205089539
8	479	0.0109091722	562	0.0295635873
9	557	0.0133032002	607	0.010090374
9	590	0.014775929	660	0.02105403
10	671	0.007328808	768	0.016273834
12	816	0.006730092	910	0.007553018
14	961	0.010041409	1080	0.00797633

2.3. Volt-Time-Curve Measurement Results

Starting from the 50% flashover voltage value, the voltage is increased with each flashover and the time from start to breakdown measured to produce voltage-time curves for the various test setup in Table I, to the procedure described in [7]. For the determination of the maximum voltage at breakdown, a dV/dt -criterion is utilized, as plotted for one of the samples in Fig. 3.

A summary of the processed results for both negative and positive polarity is depicted in Fig. 4(a) and Fig. 4(b), where a regression analysis is made for each series of

measurements and a power function used to fit the measurement samples.

The summary of both negative and positive V-t-curves in dependency of insulator discs shows a pronounced linear behaviour, as the offset of each curve increases approximately equidistant with the number of discs. However, there exists also a remarkably difference in the 9 disc measurements for HWU und UoM results, as already noted in the determination of the 50% flashover voltage. This stems from the different test setups, distribution of parasitic *capacitances* and application direction of voltage and measurement systems.

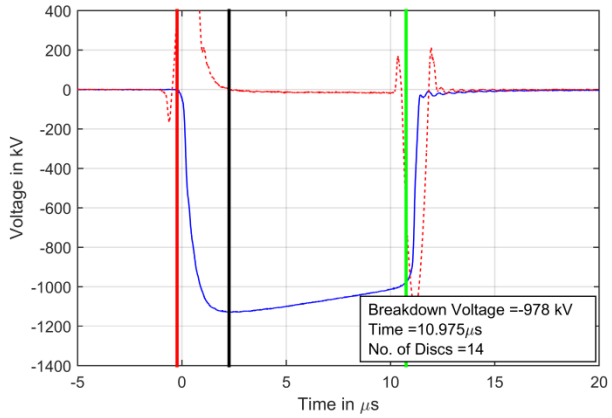

Fig. 3 *Sample plot of breakdown measurement, voltage (blue), dVdt (red dashed), tstart (red line), Vmax (black line), tbreakdown (green line)*

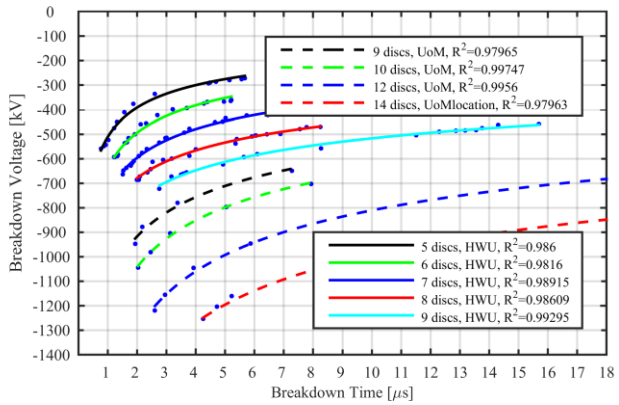

(a) Negative 1.2/50 μs waveshape

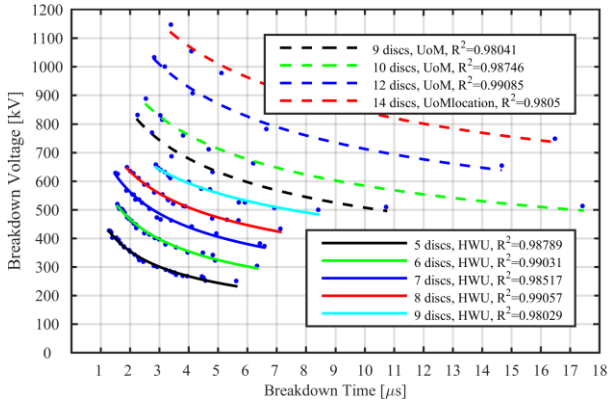

(b) Positive 1.2/50 μs waveshape

Fig. 4 *Summary of voltage-time curves*

3. Software Model of the Test Circuit

3.1. Model of Impulse Generator

As outlined in the introduction, first a software implementation of the impulse generator alongside its verification with measurements needs to be performed. In Fig. 5(a) and Fig. 5(b) the electric circuit of the 800 kV 8-stage impulse generator at HWU and 2000 kV 10-stage impulse generator at UoM are illustrated. Element values have either been taken from the manufacturers manual, measurements, analytical calculations and approximations, such as set out in [21]–[23].

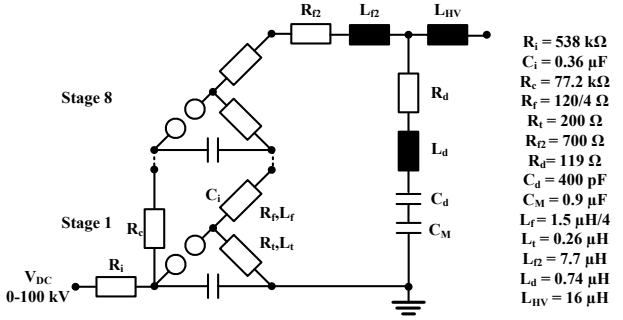

(a) *800 kV 8 stage impulse generator at HWU*

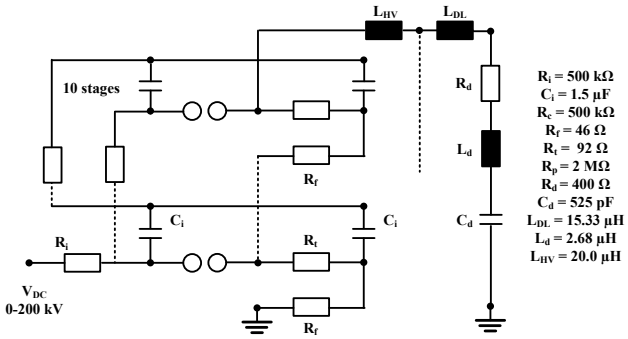

(b) *2000 kV 10 stage impulse generator at UoM*

Fig. 5 Equivalent circuits for impulse generators

The impulse generator circuit then is implemented in PSCAD/EMTDC and the software implementation voltage output at the HV side compared to various recorded shots as summarized in Fig. 6(a) and Fig. 6(b).

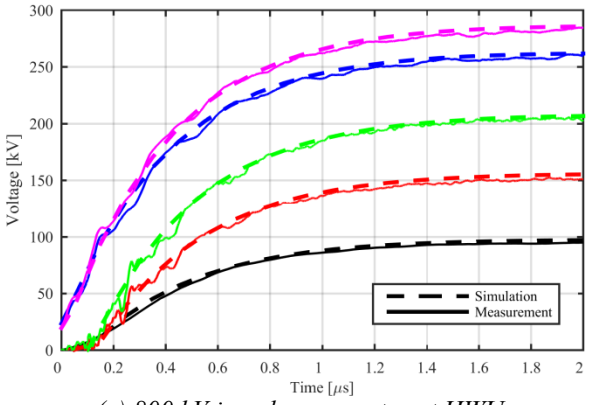

(a) 800 kV impulse generator at HWU

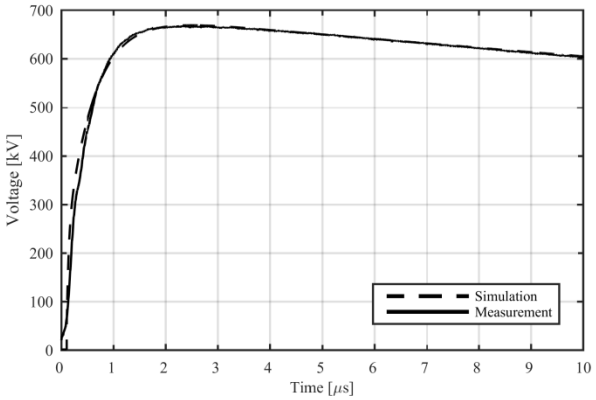

(b) *2000 kV impulse generator at UoM*

Fig. 6 *Comparison of impulse generator software model and measurement*

In general, the comparison shows a good match between simulation and measurement. However, the overlaying oscillation on the 1.2/50 µs waveform, seen in the measurements, stemming from the LV measurement circuit and recalculation to the HV side of the impulse generator voltage divider is not included in the simulations.

3.2. Leader-Progression-Model

In general, the leader progression model consists of the leader onset and the leader development process, in which the onset criterion is represented with a Volt-time area criterion in (1), with T_S, the time, $V(t)$ the voltage across the air gap and V_{AVE} the average voltage across the gap.

$$\frac{1}{T_S}\int_{t_0}^{T_S} V(t)\,\mathrm{dt} > V_{AVE} \tag{1}$$

The average voltage is derived from measurements for positive and negative polarity, calculated in (2) with variable k_1 and k_2 and D the gap length. An excerpt of values for these parameters is provided in Table 3.

$$\begin{matrix} V_{+AVE} \\ V_{-AVE} \end{matrix} > \begin{matrix} k_{1+}\cdot D + k_{2+}\,(kV) \\ k_{1-}\cdot D + k_{2-}\,(kV) \end{matrix} \tag{2}$$

Table 3 *Leader Onset Constants*

	k_1 (kV/m)	k_2 (kV)
Motoyama [6], positive polarity, air gap	400	50
Motoyama [6], negative polarity, air gap	460	150
Wang [17], positive polarity, porcelain insulator	430	190
Wang [17], negative polarity, porcelain insulator	490	90

The following leader development process is described with the average leader velocity v in m/s and average leader length x_L in meter alongside with the linear relationship of leader velocity to the pre-discharge current i in Ampere according to [6], [18] in (3) to (5), illustrated in Fig. 7 with input values in Table 4:

$$v = \begin{cases} k_{11}\cdot\left[\frac{V(t)}{D-2x_L} - E_0\right] & 0 \le x_L < \frac{D}{4} \\ k_{12}\cdot\left[\frac{V(t)}{D-2x_L} - E\left(x=\frac{D}{4}\right)\right] + v\left(x=\frac{D}{4}\right) & \frac{D}{4} \le x_L < \frac{D}{2} \end{cases} \tag{3}$$

$$x_L = \int \mathrm{v}\,dt \tag{4}$$

$$i = 2\mathrm{k}v \tag{5}$$

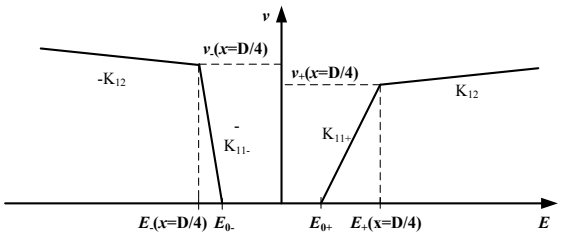

Fig. 7 *Relationship between average electric field and leader development velocity, adapted from [6]*

In case parameters from [17] are used with the formulas above, (3) and (5) have to be modified or values halved and $k_{12} = k_{11}$, because in comparison to [6], the leader progression model only includes one leader from an electrode, rather than two leaders from opposite electrodes.

Table 4 *Leader Progression Constants*

	E_0 (kV/m)	k (µC/m)	k_{11} (m^2/V·s)	k_{12} (m^2/V·s)
Motoyama [6], positive polarity	750	410	2.5	0.42
Ametani [18], positive polarity	$V(t_0)$ /D	410	3.5	0.4
Ametani [18], negative polarity	$V(t_0)$ /D	410	7.0	0.4
Wang [17], positive polarity, porcelain insulator	580	500	2.9	-
Wang [17], negative polarity, porcelain insulator	640	500	2.5	-

4. Comparison of V-t-Curves

4.1. Selection of Simulation Time-Step

To compare the V-t-curves of the measurements and the simulation model consisting of impulse generator and LPM model, the simulation time-step needs to be set. With regard to the utilization of the model in lightning simulations, the time-step is determined by the shortest line-model, generally in the range of 1E-9 to 1E-12 seconds for

line lengths in the range of 10 m to 1 m. However, during the first simulation tests, it is found that the LPM model is time-step dependent, as plotted in Fig. 8. For very short breakdown times, associated with short high current lightning impulses, a discontinuity for a time-step range of 1E-9 seconds and 1E-10 seconds is present. Additionally, at a very small time-step 1E-12 seconds the V-t-curves tend to shift upwards due to the lower speed increment in (4). For the range of arc-gaps simulated, it is found that the results are consistent for time-steps in the range of 5E-11 to 5E-12 seconds. Therefore a time-step of 5E-11 is chosen for all further simulations.

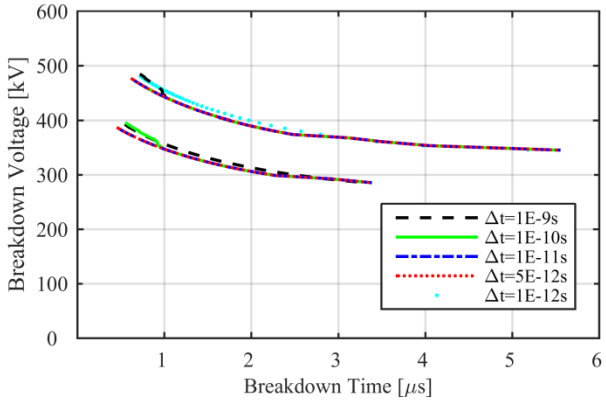

Fig. 8 *Time-step dependency of flashover results for 0.43 cm and 0.57 cm arc gap, HWU impulse generator*

4.2. V-t-curve Comparison for Flashover Tests

In general, the LPM parameters are directly determined with measured current and leader velocity, see [6], [17]. However, measurements are only available in form of breakdown measurements of voltage. Therefore, it is decided to conduct a parameter study and determine parameters based on the best fit to the V-t-curve measurements.

At first, the parameter set from Motoyama in Table III and Table IV is compared to the measured V-t-curves to identify the differences for a start point of the parameter study. To record both the voltage at breakdown and time to breakdown, an implementation of the dV/dt-criterion, explained in section II, C is implemented to align the evaluation procedure of simulation and measurement.

In Fig. 9(a) and Fig. 9(b) the V-t-curves resulting from simulations with a 2000 kV impulse generator are plotted together with the V-t-curve points resulting from the experiments.

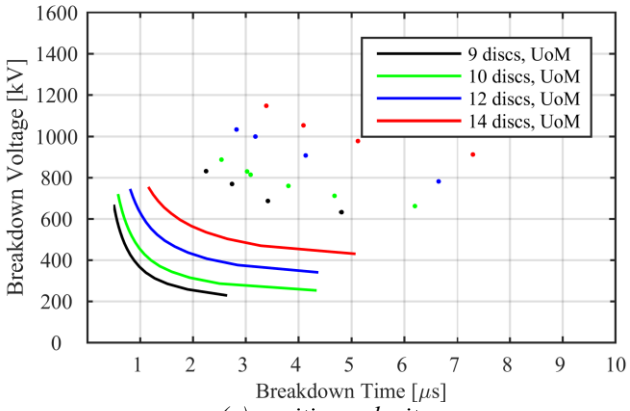

(a) positive polarity

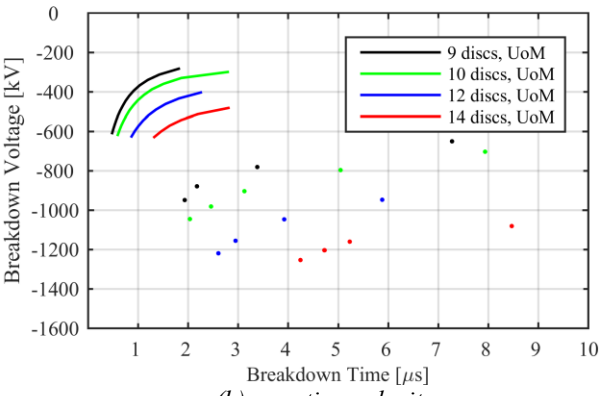

(b) negative polarity

Fig. 9 *Comparison of voltage-time curves of Cap-and-pin insulator string with arcing horns obtained from measurements to the LPM simulation with Motoyama parameters for air gaps, 2000 kV impulse generator UoM*

A comparison of the V-t-curves shows, that the Motoyama parameters underestimate the real performance of the cap-and-pin glass insulators with arcing horns and need to be adjusted. In this respect, a systematic approach to determine the influence of each parameter in the LPM on the simulated V-t-curve is taken. The result of this approach is depicted in Fig. 10, which reveals that each parameter features a dominant influence on a property of the V-t-curve, and a minor influence on the whole shape of the V-t-curve.

The velocity parameters K_{11} and K_{12} shift the V-t-curve to longer breakdown times in case of decreasing their values, but also stretch the curve to longer breakdown times. The charge parameter K_0, which mainly determines the pre-discharge current, decreases the slope of the V-t-curve, but also the maximum peak voltage, when it is decreased. Parameters k_1 and k_2 shift the curve to lower breakdown voltages, but also compress the V-t-curve to lower breakdown time values when decreased.

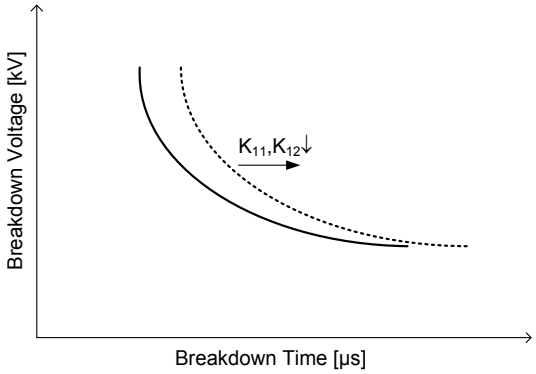

(a) Parameters K11 and K12

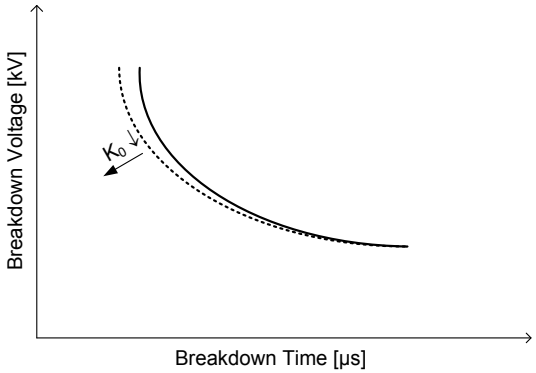

(b) Parameter K0

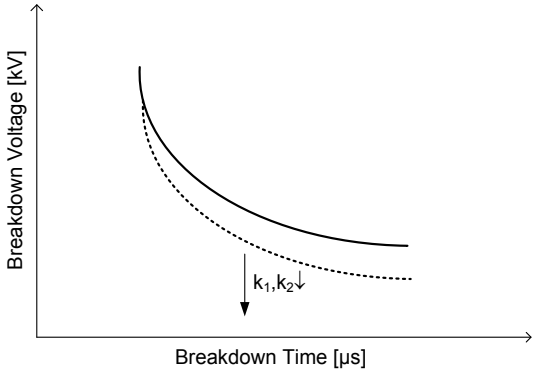

(c) Parameter k1 and k2

Fig. 10 *Main influence of LPM parameters on V-t-curve*

Furthermore, it is found that there exists a range of parameter sets to fit the measured V-t-curve, which demands for further criteria for curve fitting. Since the information available is limited to the measured voltage and breakdown measurements, only the criterion of maximum voltage is available. Concluding from the influence of parameter K_0 on the peak voltage in the previous paragraph, the maximum voltage - breakdown time (V_{max}-t) –Curve is utilized in addition to the V-t-curve for a parameter fitting of the LPM.

For a first parameter determination, the numbers of variables to be adjusted is reduced in setting parameter $K_{12} = K_{11}$. A manual adjustment can readily be performed in the following steps:

- Adjust k_1 and k_2 to get an approximate fit for the horizontal line of the V-t-curve
- Adjust K_{11} to shift the V-t-curve vertically
- Adjust K_0 to get a fit for the upper part of the V-t-curve
- Iterate above steps until a reasonable fit is achieved

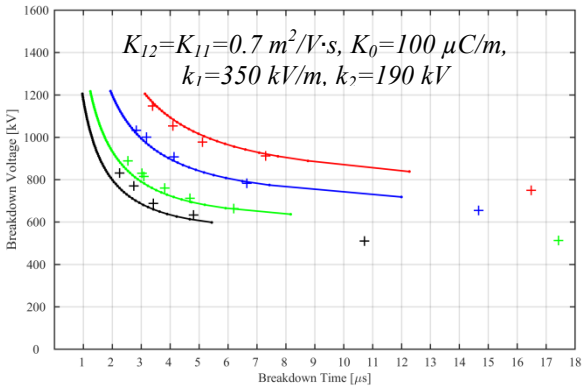

(a) Voltage-time curve positive polarity

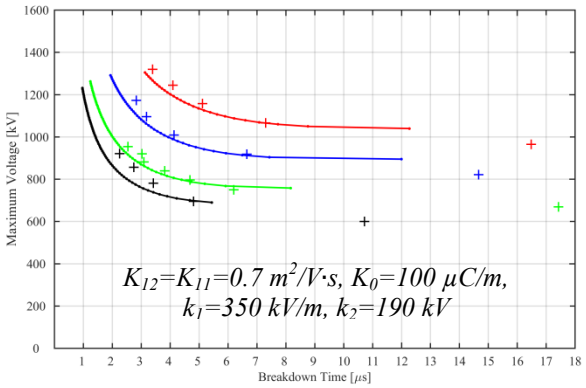

(b) Maximum voltage-time curve positive polarity

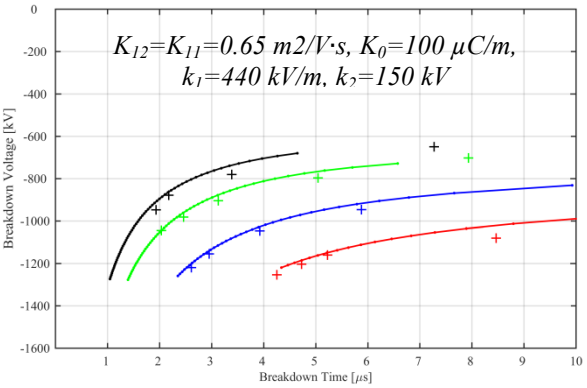

(c) Voltage-time curve negative polarity

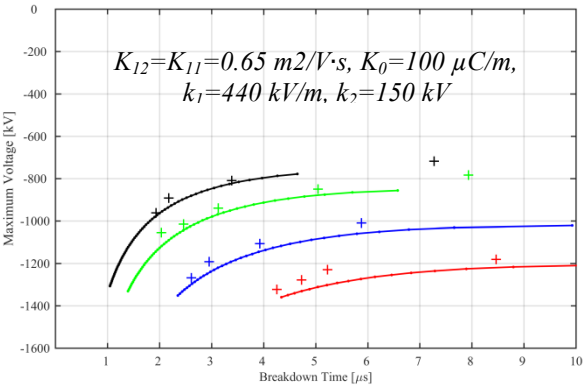

(d) *Maximum voltage-time curve negative polarity*

Fig. 11 *Comparison of V-t-curve measurements and simulation for 2000 kV impulse generator with K12=K11*

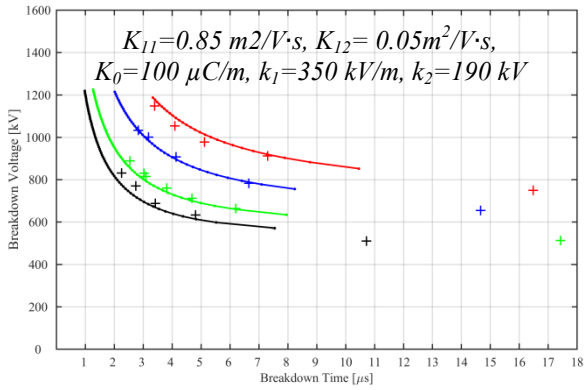

(a) *Voltage-time curve positive polarity,*

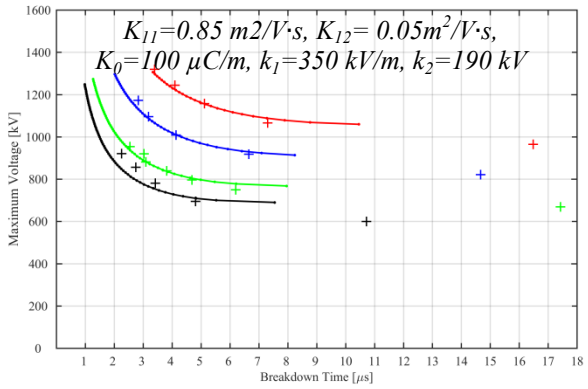

(b) *Maximum voltage-time curve positive polarity*

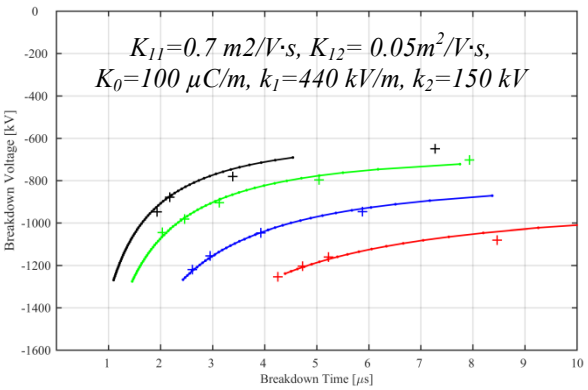

(c) *Voltage-time curve negative polarity*

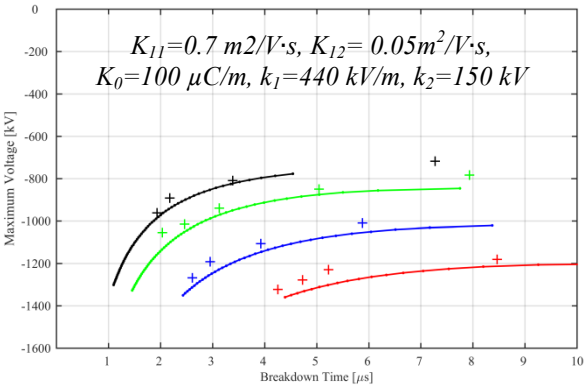

(d) *Maximum voltage-time curve negative polarity*

Fig. 12 *Comparison of V-t-curve measurements and simulation for 2000 kV impulse generator with K12≠K11*

In Fig. 11 a reasonable fit for the measured positive and negative V-t-curve is found for the LPM parameter set with K_{12}=K_{11}, respectively. In the described iterative process to find a parameter set, which fits both the V-t-curve as well as the V_{max}-t-curve a state is reached, where variations in the parameter set either lead to a better fit of the V-t-curve or V_{max}-t-curve, but not both. The corresponding parameter set results in the curve fitting in Fig. 11.

To investigate if the fit to the measured V-t- and V_{max}-t-curve can be improved, the variable K_{12}≠K_{11} is taken into consideration in the simulations and the previously described procedure repeated. In Fig. 12 the results of the curve-fitting procedure are plotted for both positive and negative polarity.

5. Summary and Conclusion

In this paper laboratory flashover tests on a cap-and-pin glass insulator string with arcing horns are conducted with a various number of discs to determine the 50% flashover voltage and the associated volt-time (V-t) curves. A comparison of the measured V-t-curves with generated V-t-curves from an implementation of the impulse generator and physical leader-progression model in EMT using standard parameters for an air gap show large differences.

Since only the voltage plots are available for an adjustment of the LPM's parameters to fit the measured V-t-curves, a curve-fitting procedure, taking also the maximum voltage-breakdown time curve into account was applied. The determined LPM parameters are in the same range as published results for porcelain insulators without arcing horns. Although a reasonable fit for both the breakdown voltage-time-curve and maximum voltage-time-curve can be found, deviations from the measured curves still exist. The main problem of curve-fitting is that no definite criterion for the breakdown can be determined. The dV/dt-criterion used may be the best option to determine the breakdown time, but due to the pre-discharge current, where no fast cut-off of voltage in the plots exists, the determination of breakdown voltage leaves some degree of freedom. Furthermore, inductive effects during the breakdown process and the electric arc itself cannot be modelled in detail, which adds some further inaccuracy to the determination of the LPM parameters, when velocity and current measurement during the breakdown process are not available. However, as reported in [6], [7], [17] short-tail waveshapes as encountered during a lightning strike at the insulator with arcing horns have higher breakdown voltage than the 1.2/50µs waveshape, applied in this work, which adds a safety margin and enables the application of the determined LPM parameters on a worst-case basis. Although breakdown experiments are conducted only for arcing horn lengths up to 1.70 m, the equidistant shift of the V-t-curves in dependency of the number of insulator discs, justifies the LPM parameter usage for longer arcing horn length.

6. Acknowledgments

This work is supported by Faiva Wadawasina from Scottish and Southern Energy Power Distribution, Perth, Scotland (SSEPD) under the OFGEM Network Innovation Allowance (NIA_SHET_0011).

7. References

[1] T. Pham and S. Boggs, “Flashover model of arcing horn in transient simulation,” *Conference Record of IEEE International Symposium on Electrical Insulation*, pp. 8–11, 2010.

[2] I. Cotton, A. Kadir, and M. Abidin, “A randomised leader progression model for backflashover studies,” *European Transactions on Electrical Power*, vol. 18, pp. 709–724, 2008.

[3] IEEE Task Force on Fast Front Transients, “Modeling guidelines for fast front transients,” *IEEE Transactions on Power Delivery*, vol. 11, no. 1, pp. 493–506, 1996.

[4] M. Darveniza and a. E. Vlastos, “Generalized integration method for predicting impulse volt-time characteristics for non-standard wave shapes - a theoretical basis.,” *IEEE Transactions on Electrical Insulation*, vol. 23, no. 3, pp. 373–381, 1988.

[5] D. Kind, “Die Aufbaufläche bei Stoßbeanspruchung technischer Elektrodenanordnungen in Luft,” *Ph.D. Dissertation TU München*. 1957.

[6] H. Motoyama, “Experimental study and analysis of breakdown characteristics of long air gaps with short tail lightning impulse,” *IEEE Transactions on Power Delivery*, vol. 11, no. 2, pp. 972–979, 1996.

[7] A. Pigini and G. Rizzi, “Performance of large air gaps under lightning overvoltages: experimental study and analysis of accuracy predetermination methods,” *IEEE Transactions on Power Delivery*, 1989.

[8] T. Shindo, Y. Aoshima, I. Kishizima, and T. Harada, “A study of predischarge current characteristics of long air gaps,” *IEEE Transactions on Power Apparatus and Systems*, vol. 78, no. 11, pp. 3262–3268, 1985.

[9] T. Shindo and T. Suzuki, “A new calculation method of breakdown voltage-time characteristics of long air gaps,” *IEEE Transactions on Power Apparatus and Systems*, 1985.

[10] T. Ueda, S. Neo, and T. Funabashi, “Flashover model for arcing horns and transmission line arresters,” *International Conference on Power Systems Transients*, 1995.

[11] CIGRE Working Group 33.01, “Guide to procedures for estimating the lightning performance of transmission lines,” 1991.

[12] CIGRE Working Group 33.02, “Guidelines for Representation of Network Elements when Calculating Transients,” 1990.

[13] W. G. 33. 0. CIGRE, “Guidelines for the evaluation of the dielectric strength of external insulation,” 1992.

[14] IEC/TR 60071-4: 2004, “Insulation co-ordination - Part 4: Computational guide to insulation co-ordination and modelling of electrical networks,” 2004.

[15] Z. Datsios and P. Mikropoulos, “Implementation of leader development models in ATP-EMTP Using a type-94 circuit component,” *Internation Conference on Lightning Protection (ICLP)*, 2014.

[16] T. Mozumi, Y. Baba, M. Ishii, N. Nagaoka, and A. Ametani, “Numerical electromagnetic field analysis of archorn voltages during a back-flashover on a 500-kV twin-circuit line,” *IEEE Transactions on Power Delivery*, vol. 18, no. 1, pp. 207–213, 2003.

[17] X. Wang, Z. Yu, and J. He, “Breakdown Process Experiments of 110- to 500-kV Insulator Strings Under Short Tail Lightning Impulse,” *IEEE Transactions on Power Delivery*, vol. 29, no. 5, pp. 2394–2401, 2014.

[18] A. Ametani, N. Nagaoka, K. Ueno, and T. Funabashi, “Investigation of flashover phases in a lightning surge by new archorn and tower models,” *IEEE/PES Transmission and Distribution Conference and Exhibition*, vol. 2, pp. 0–5, 2002.

[19] A. Ametani and T. Kawamura, “A method of a lightning surge analysis recommended in Japan using EMTP,” *IEEE Transactions on Power Delivery*, vol. 20, no. 2 I, pp. 867–875, 2005.

[20] M. Kizilcay, “Mitigation of Back-Flashovers for 110-kV Lines at Multi-Circuit Overhead Line Towers,” *Proceedings of the International Conference on Power Systems Transients*, 2009.

[21] W. Hauschild and E. Lemke, *High-Voltage Test and Measuring Techniques*. 2014.

[22] A. Schwab, *Hochspannungsmesstechnik - Messgeraete und Messverfahren*. 2011.

[23] A. Küchler, *Hochspannungstechnik*. Berlin, Heidelberg: Springer Berlin Heidelberg, 2009.